FEBS Open Bio 4 (2014) 200–212

FEBS openbio

journal homepage: www.elsevier.com/locate/febsopenbio

Similarities and differences in the biochemical and enzymological properties of the four isomaltases from *Saccharomyces cerevisiae*

Xu Deng [a,b,c,1], Marjorie Petitjean [a,b,c,1], Marie-Ange Teste [a,b,c], Wafa Kooli [a,b,c], Samuel Tranier [d,e], Jean Marie François [a,b,c], Jean-Luc Parrou [a,b,c,*]

[a] CNRS, UMR5504, F-31400 Toulouse, France
[b] INRA, UMR792 Ingénierie des Systèmes Biologiques et des Procédés, F-31400 Toulouse, France
[c] Université de Toulouse, INSA, UPS, INP, LISBP, 135 Avenue de Rangueil, F-31077 Toulouse, France
[d] CNRS, IPBS, Département de Biologie Structurale et Biophysique, 205 Route de Narbonne, BP 64182, F-31077 Toulouse, France
[e] Université de Toulouse, UPS, IPBS, F-31077 Toulouse, France

ARTICLE INFO

Article history:
Received 23 December 2013
Revised 29 January 2014
Accepted 10 February 2014

Keywords:
Yeast
α-Glucosidase
Isomaltase
Isomaltose
Maltose
Substrate ambiguity
Substrate inhibition
Thermostability
Proline substitution

ABSTRACT

The yeast *Saccharomyces cerevisiae IMA* multigene family encodes four isomaltases sharing high sequence identity from 65% to 99%. Here, we explore their functional diversity, with exhaustive *in-vitro* characterization of their enzymological and biochemical properties. The four isoenzymes exhibited a preference for the α-(1,6) disaccharides isomaltose and palatinose, with Michaëlis–Menten kinetics and inhibition at high substrates concentration. They were also able to hydrolyze trisaccharides bearing an α-(1,6) linkage, but also α-(1,2), α-(1,3) and α-(1,5) disaccharides including sucrose, highlighting their substrate ambiguity. While Ima1p and Ima2p presented almost identical characteristics, our results nevertheless showed many singularities within this protein family. In particular, Ima3p presented lower activities and thermostability than Ima2p despite only three different amino acids between the sequences of these two isoforms. The Ima3p_R279Q variant recovered activity levels of Ima2p, while the Leu-to-Pro substitution at position 240 significantly increased the stability of Ima3p and supported the role of prolines in thermostability. The most distant protein, Ima5p, presented the lowest optimal temperature and was also extremely sensitive to temperature. Isomaltose hydrolysis by Ima5p challenged previous conclusions about the requirement of specific amino acids for determining the specificity for α-(1,6) substrates. We finally found a mixed inhibition by maltose for Ima5p while, contrary to a previous work, Ima1p inhibition by maltose was competitive at very low isomaltose concentrations and uncompetitive as the substrate concentration increased. Altogether, this work illustrates that a gene family encoding proteins with strong sequence similarities can lead to enzyme with notable differences in biochemical and enzymological properties.

1. Introduction

Isomaltases (EC 3.2.1.10) are oligo-α-1,6-glucosidases that hydrolyze the α-1,6-glycosidic linkages at the non-reducing end with retention of the anomeric configuration. They belong to the 'α-amylase' family of enzymes, which includes proteins with almost 30 different specificities, *e.g.* retaining glycoside hydrolases and transferases acting on α-glucosidic substrates such as starch, dextran, sucrose, etc. [1]. Isomaltases have been classified in the subfamily 31 of the glycoside hydrolase family 13 (GH13_31, [2] according to the CAZy database that assigns carbohydrate-active enzymes into GH families sharing structural fold and stereochemical mechanism (http://www.cazy.org/, [3]). Contrary to α-1,6-glucosidases such as the dextran glucosidase from *Streptococcus mutans* (SmDG) that act on long-chain isomaltooligosaccharides (IMOs) [4], isomaltases preferentially cleave shorter IMOs [1].

Abbreviations: DSF, differential scanning fluorimetry; GH, glycoside hydrolase; IMO, isomalto-oligosachharide; α-MG, α-methylglucoside; SmDG, dextran glucosidase from *Streptococcus mutans*

* Corresponding author. Address: Laboratoire d'Ingénierie des Systèmes Biologiques et des Procédés, INSA, CNRS UMR5504, UMR INRA 792, 135 Avenue de Rangueil, F-31077 Toulouse Cedex 4, France. Tel.: +33 561 559 423; fax: +33 561 559 400.
E-mail address: parrou@insa-toulouse.fr (J.-L. Parrou).
URL: http://www.lisbp.fr/fr/index.html (J.-L. Parrou).
[1] Equal contribution.

http://dx.doi.org/10.1016/j.fob.2014.02.004

Previous works on purified α-glucosidases from baker's and brewer's yeasts [5–12] showed that isomaltase hydrolyses isomaltose and α-methylglucoside (α-MG) but not maltose, whereas maltase hydrolyses maltose but not isomaltose and α-MG. A gene encoding an isomaltase was first isolated from a *Saccharomyces cerevisiae* cDNA library and turned out to be *YGR287c* encoding a 589 amino acid protein able to hydrolyze isomaltose and α-MG but totally inactive on maltose [5]. The crystal structure of this protein was solved, underlying the importance of some amino acids in the structure of the active site and explaining its specificity for isomaltose [13,14]. More recently, we found with another group that the yeast S288c genome actually bears five related coding sequences located in the subtelomeres of different chromosomes that compose the *IMA* multigene family [6,15]. Two of them, namely *IMA3* and *IMA4* are strictly identical and encode the same protein (Ima3p, *id*. Ima4p). The Ima2 and Ima3 proteins exhibit only 3 different amino acids, while the most distant gene *IMA5* encodes a protein sharing 65% sequence identity with the remaining members of the family (Fig. S1). All four Ima proteins possess the highly conserved regions of the GH13 family (consensus sequences I to IV), which include the catalytic triad (Asp215, nucleophile; Glu277, proton donor and Asp352, transition-state stabilizer) and the valine residue identified as a key signature of α-1,6 hydrolytic activity (Val216 from Ima1p) [5].

Strong discrepancies were noticed in published data, *i.e.* substrates specificities and kinetic parameters of the isomaltase from the yeast *S. cerevisiae* [8–12] and from closely related yeast species [8,16,17], probably because enzymological properties have been determined from different isoenzymes or purified fractions that contained a mix of these isoenzymes. Current facilities for gene expression and protein purification allowed us to carry out a detailed biochemical and enzymological characterization of the four isomaltases encoded by the yeast *S. cerevisiae* [6,15], including a revision of the biochemical properties of the protein encoded by *IMA1* [5,13,14]. Targeted mutagenesis further provided key results to understand the role of important amino acid residues in substrate specificities and thermostability of these Ima proteins.

2. Results

2.1. Biochemical characterization of the 4 isomaltases

Using pNPG as a substrate, the optimum pH of the four isomaltases was determined in the citrate–potassium phosphate buffer (pH 2.6–8.0) and in the sodium phosphate buffer (pH 7.0–9.0). The four proteins showed similar pH profiles with an optimum between 7 and 8 (Table 1), no measurable activity below pH 5.0 and a drop of activity above pH 8.0. This optimum pH was in the range of the intracellular pH of yeast cells [18]. The optimum temperature for activity was slightly more discriminant than pH_{opt}. The Ima5p was the most singular with an optimal activity at 36 °C, whereas the optimum temperature was 43 °C for Ima2p and 46 °C for both Ima1p and Ima3p (Table 1). At higher temperatures, the activity abruptly dropped with a complete loss of activity above 45 °C for Ima5p and above 55 °C for the three other enzymes.

The influence of various compounds and metal ions was also tested (Fig. S2). Only iron under its ferric form significantly inhibited the four enzymes, especially Ima1p with only 8% residual activity in the presence of 5 mM Fe^{3+}. Conversely, the activity of this isoenzyme was slightly enhanced by Mg^{2+} (5 mM) and Mn^{2+} (1 mM). Since Ima proteins possess a calcium binding site ([13,14], Fig. S1), we tested the effects of adding Ca^{2+} or on the contrary EDTA to chelate this cation that is potentially buried in its binding site. None of the isoforms was affected by the addition of Ca^{2+} and although Ima3p was slightly inhibited by the addition EDTA, our results suggested that calcium ions were not implicated in yeast isomaltase activity. From a list of many other organic and inorganic compounds, we found that all isomaltases were highly sensitive to Tris with 90% inhibition of the activity in the presence of only 5 mM and, contrary to a previous work [9], to ammonium ions with 25–85% inhibition in the presence of 1.25–10% $(NH_4)_2SO_4$ in the reaction mixture, respectively (not illustrated).

We finally searched for stabilization conditions for long term storage of our purified enzyme preparations (*e.g.* 24 h storage or more). The addition of glycerol up to 40%, Tris up to 20 mM or 10% $(NH_4)_2SO_4$, removal of the imidazole after protein purification, decrease of pH to 6.0, storage at 4, −20 or −80 °C did not improve the stabilization and long term preservation of protein activity (data not shown). As a consequence, we carried out all our enzymatic analysis from freshly purified Ima proteins.

2.2. Temperature stability of the different isoenzymes

Since our assay was based on the continuous monitoring of *p*-nitrophenyl from pNPG at 405 nm on a spectrophotometer, we noticed that the kinetic curves declined rapidly with time, even when the assay was carried out under optimal conditions, suggesting that the Ima proteins were subjected to inactivation or denaturation. Therefore, a time-dependent heat inactivation analysis at different temperatures was carried out for each enzyme, showing an exponential decay of enzyme activity that correlated with irreversible thermal deactivation process (Fig. S3A). This behaviour allowed calculating the half-life ($t_{1/2}$) for each enzyme and at different temperatures (see summarizing Table 1 and Fig. S3B). The half-life value at 37 °C was 3 min for Ima5p, 23 min for Ima3p and 27 min for both Ima2p and Ima1p. When the assay temperature was set at 40 °C, the half-life dropped to 1 min for Ima5p, 8 min for Ima3p and 18 min for both Ima1p and Ima2p, illustrating the dramatic sensitivity of isomaltases to increasing temperature. Finally, since the binding of calcium has been reported to positively affect proteins thermal stability [19,20], we also evaluated the stability of the different Ima isoforms in the presence of EDTA. We got strictly identical thermal denaturation curves for kinetics up to 30 min, at different temperatures, with and without EDTA (data not shown), indicating that this compound did not affect isomaltase thermostability.

DSF experiments strengthened the different sensitivity of the Ima proteins towards temperature, as the melting temperatures (T_m) of the purified proteins determined at pH 7.0 were around 36, 39 and 46 °C for Ima5p, Ima3p and Ima1p or Ima2p, respectively (Table 1). These values were remarkably influenced by the pH value since a decrease by only one pH unit (pH 6) increased the T_m by *approx*. 9 °C, whereas an increase by one unit (pH 8) decreased the T_m by 5 °C for Ima1p and by 13 °C for Ima2p. In deep contrast, the T_m of Ima5p was almost insensitive to pH (Table 1). Also, the T_m of these 4 proteins was increased by about 5 °C in the presence of Tris 5 mM (assay at pH 7.0, results not shown).

2.3. Importance of proline in the thermal stability of Ima3p

While Ima2p and Ima3p only differ in their primary sequence by three amino acids (A54/T54, P240/L240 and Q279/R279 for Ima2p *vs.* Ima3p, respectively; see Fig. S1), the remarkable difference in their thermal stability prompted us to investigate the importance of these amino acids residues. We initially focused our attention on the proline at position 240 since it was already reported that proline residues greatly influence protein thermostability [21–24]. Accordingly, we found that the Ima3p_L240P variant led to a significant increase of the half-life of the protein (Table 1 and Fig. S3), from 23.2 (Ima3p) to 26.5 min (L240P variant) when the proteins were incubated at 37 °C, and from 7.6 to

Table 1
Biochemical parameters of the four isomaltases.

Enzyme	pH_{opt}	T_{opt} (°C)	$t_{1/2}$ (min)			T_m (°C)		
			37 °C	40 °C	42 °C	pH 6	pH 7	pH 8
Ima1p	7	46	26.1 ± 1.7	17.6 ± 1.7	nd	55.5 ± 0.6	46.6 ± 0.7	41.6 ± 0.2
Ima2p	7.6	43	27.4 ± 1.6	18.5 ± 1.6	11.2 ± 0.7	55.1 ± 0.2	46.2 ± 0.8	33.2 ± 0.6
Ima3p	8	46	23.2 ± 1.4	7.6 ± 0.9	2.9 ± 0.5	47.0 ± 0.3	38.8 ± 0.5	29.9 ± 0.3
Ima5p	7	36	2.9 ± 0.4	0.8 ± 0.1	nd	36.6 ± 0.4	36.3 ± 0.4	35.7 ± 0.5
Ima3p_R279Q	nd[a]	nd	9.5 ± 1.7	2.0 ± 0.3	nd	nd	37.6 ± 0.8	nd
Ima3p_L240P	nd	nd	26.5 ± 2.2	16.2 ± 1.8	8.5 ± 1.3	nd	39.7 ± 0.4	nd

pH_{opt}: pH optimum; T_{opt}: temperature optimum; $t_{1/2}$: half-life; T_m: Melting temperature.
[a] Not determined. In all cases, pNPG 5 mM was used as the substrate. Half-life and T_m values reported as the mean ± 2 SEM. Samples size and distribution (average of 7 independent assays for each temperature, see Fig. S3B) allowed applying a Student's *t*-test for some pairs of proteins (statistically relevant differences with a confidence level of 95% when *p*-value < 0.05): Ima3p_L240P *vs.* Ima3p: *p*-value = 0.022 at 37 °C; Ima3p_L240P *vs.* Ima2p: *p*-value = 0.530 at 37 °C, 0.087 at 40 °C and 0.003 at 42 °C. The melting temperature (T_m) was determined by Differential Scanning Fluorimetry (DSF) from five independent replicates for each protein, which allowed applying a Student's *t*-test (confidence level of 95%): Ima3 *vs.* Ima3_L240P: *p*-value = 0.016; Ima3 *vs.* Ima3_R279Q: *p*-value = 0.084.

16.2 min when the assay was carried out at 40 °C. These $t_{1/2}$ values of the Ima3p_L240P variant were undistinguishable from those of Ima2p, setting the importance of this proline substitution in enhancing thermal stability of Ima3p. However, this statement could be qualified as this substitution was not enough to recover the full thermostability properties of Ima2p. First, the $t_{1/2}$ of Ima3p_L240P variant was lower than Ima2p (8.5 *vs.* 11.2 min) when the proteins were incubated at 42 °C. Second, the T_m value of the Ima3p_L240P variant only increased by 1 °C (from 38.8 °C for Ima3p to 39.7 °C for Ima3p_L240P), which remained much lower than the T_m of Ima2p (46.2 °C). These results altogether indicated that the proline residue at position 240 in Ima2p, although central, was not the sole determinant of the difference in thermal stability between Ima2p and Ima3p.

2.4. Substrates specificities and determination of catalytic constants

Substrates specificities of purified yeast isomaltases were assessed using a set of di- or trisaccharides with different α-glycosidic linkages and variable composition (Table 2). As expected, the 4 isomaltases were only active on the α-D-glucopyranosides, since no release of pNP was observed using β-pNPG as substrate. They were preferentially active on disaccharides bearing a α-1,6 linkage, either between two glucose units (isomaltose, activity set at 100%) or between glucose and fructose moieties (palatinose), for which relative activities ranged from 60% (Ima5p) to 137% (Ima2p). They were inactive on melibiose (*O*-α-D-galactosyl-(1→6)-α-D-glucose, not shown), which indicated that a glucose moiety was required at the non-reducing end of the disaccharide for recognition and binding in the active site pocket. Interestingly, Ima proteins also exhibited α-1,2 glucosidase activity on sucrose and kojibiose, but with great disparity in the activity between the different isoenzymes. The activity on sucrose was *approx.* 35% relative to isomaltose for Ima1p and Ima2p, and it was reduced to 2% for Ima5p. Interestingly, Ima3p exhibited lower affinity but much higher V_{max} on sucrose than for isomaltose and it was totally inactive on kojibiose. We also found that the four proteins could also cleave the α-1,3 linkage of nigerose and turanose and also, with the exception of Ima3p, the α-1,5 linkage of leucrose with an average activity of 10–15% relative to that found on isomaltose. In contrast, all Ima proteins were totally inactive on maltose, but two of them, Ima2p and Ima5p showed very low, albeit

Table 2
Substrate specificity of purified isomaltases.

Substrate	Linkage	Specific activities (μmol/min/mg)					
		Ima1p	Ima2p	Ima3p	Ima5p	Ima3pL240P	Ima3pR279Q
α-pNPG	4-Nitrophenyl α-D-glucopyranoside	5.8 (10)	7.7 (14)	3.9 (54)	10 (15)	5.5	8.5
β-pNPG	4-Nitrophenyl β-D-glucopyranoside	0	0	0	0	nd[a]	nd
α-MG	α-Methylglucopyranoside	52 (87)	55 (102)	11 (153)	0 (0)	6.5	50
Disaccharides (Glc → Glc)							
Trehalose	*O*-α-D-Glucosyl-(1→1)-α-D-glucose	0	0	0	0	nd	nd
Kojibiose	*O*-α-D-Glucosyl-(1→2)-α-D-glucose	7.7 (13)	6.9 (13)	0	2.5 (4)	nd	nd
Nigerose	*O*-α-D-Glucosyl-(1→3)-α-D-glucose	6.5 (11)	6.8 (13)	2.5 (35)	4.2 (6)	nd	nd
Maltose	*O*-α-D-Glucosyl-(1→4)-α-D-glucose	0	0	0	0	nd	nd
Isomaltose	*O*-α-D-Glucosyl-(1→6)-α-D-glucose	60 (100)	54 (100)	7.2 (100)	65 (100)	2.2	29
Disaccharides (Glc → Fru)							
Sucrose	*O*-α-D-Glucosyl-(1→2)-β-D-fructose	18.6 (31)	19.7 (36)	10.2 (142)	1.2 (2)	11.2	22
Turanose	*O*-α-D-Glucosyl-(1→3)-D-fructose	4.3 (7)	3.5 (6)	1.8 (25)	1.2 (2)	nd	nd
Maltulose	*O*-α-D-Glucosyl-(1→4)-D-fructose	0	0.53 (1)	0	0.36 (1)	nd	nd
Leucrose	*O*-α-D-Glucosyl-(1→5)-D-fructose	8.6 (14)	8.6 (16)	0	1.1 (2)	0	1.5
Palatinose	*O*-α-D-Glucosyl-(1→6)-D-fructose	52 (87)	74 (137)	5 (69)	39 (60)	2.8	33
Trisaccharides							
Maltotriose	*O*-α-D-Glucosyl-(1→4)-α-D-glucosyl-(1→4)-D-glucose	3.5 (6)	3.4 (6)	0	3.4 (5)	nd	nd
Isomaltotriose	*O*-α-D-Glucosyl-(1→6)-α-D-glucosyl-(1→6)-D-glucose	7.9 (13)	7.6 (14)	0	8.6 (13)	nd	nd
Melezitose (Glc → Suc)	*O*-α-D-Glucosyl-(1→3)-β-D-fructosyl-(2→1)-D-glucose	0	0	0	0	nd	nd
Panose	*O*-α-D-Glucosyl-(1→6)-α-D-glucosyl-(1→4)-D-glucose	3.1 (5)	2.9 (5)	0	11 (17)	0	3.1

Specific enzyme activities were determined with 100 mM of substrate, except for pNPG that was assayed at 5 mM, from an average of five independent experiments to get SEM ⩽ 10% of the mean value. All reactions were carried out in the citrate–potassium phosphate buffer, pH 7, 30 °C.
[a] Not determined. Between brackets: relative activity, taking as a reference for each enzyme the velocity on isomaltose (set to 100).

reproducible activity on maltulose, indicating that a statement on the total absence of reactivity on α-1,4 linkages must be nuanced. With the exception of Ima3p, the three other Ima proteins also displayed a measurable activity on some trisaccharides including isomaltotriose and panose, but also maltotriose (*approx*. 5% relative to isomaltose), which contrasted with the absence of activity on the α-1,4 linkage of maltose. No activity could be detected with longer malto-oligosaccharides such as maltopentaose or maltoheptaose (data not shown).

As already pointed out for the difference in the thermostability between Ima2p and Ima3p, we investigated which of the three amino acids could account for the difference in substrate specificities and activities between these two proteins. While the Ima3p_L240P variant presented the same characteristics as Ima3p, the R279Q mutation allowed recovering substrate specificities and specific activities close to those of Ima2p (Table 2). Similarly, we investigated whether the replacement of the triplet VGI in Ima5p (residues 278-280) by MQH, which is the only difference between Ima5p and Ima1/2/3p when comparing consensus regions I–IV of the GH13 family (Fig. S1), could swap the enzymological properties of Ima5p to those of Ima1p. Contrary to expectation, the VGI to MQH mutation totally abolished the catalytic activity of this isoenzyme (data not shown), whatsoever the substrate used.

2.5. Comparative analysis of the kinetic properties of the 4 isomaltases

The kinetic properties of the 4 isomaltases were determined on substrates that yielded to substantial activities. As is shown in Fig. 1, the 4 Ima proteins displayed Michaëlis–Menten kinetics towards isomaltose with a clear inhibition at high substrate concentration (Fig. 1). As can be seen in the overview of velocity-substrate profiles (Fig. 2 and Fig. S4A–D), Michaëlis–Menten kinetics were also recorded with other substrates including α-MG, palatinose, panose, sucrose and isomaltriose. Inhibitions by excess of substrate were observed for palatinose and to a lesser extend for α-MG, except for Ima3p which did not display this behaviour. Similarly, all Ima isoforms were inhibited at high concentration of α-pNPG (Fig. S5), the artificial substrate of these enzymes, with a drop of activity from 10% for Ima1p and Ima5p to 33% for Ima3p when the substrate concentration increased to 10 mM. As can be seen in Table 3, the catalytic efficiency (k_{cat}/K_m [25]) of Ima proteins was much higher for α-pNPG than for the natural substrates, including isomaltose (from 3-fold for Ima1/2/5p to 50-fold for Ima3p), which was explained by much lower affinity constants (*approx*. 0.5 mM for α-pNPG as compared to 10–200 mM for natural substrates).

The catalytic properties of Ima1p and Ima2p on the different substrates were remarkably similar, and the higher activity of Ima2p on palatinose, especially when decreasing substrate concentration, was the only differentiating feature between these two proteins (Fig. 2B). The higher k_{cat}/K_m values for isomaltose and palatinose than for sucrose, isomaltotriose and panose, clearly demonstrated the preference of these two isomaltases for disaccharides with a α-1,6 glycosidic linkage. However, the extremely low affinity of both proteins for sucrose (K_m ~145 mM) did not impair quite significant cleavage as soon as this sugar was provided at high concentration. With only 65% sequence identity with Ima1p, Ima5p showed comparable catalytic constants and patterns on substrates with α-1,6 linkage such as isomaltose, palatinose but also isomaltotriose (Table 3 and Fig. 2). As clearly illustrated in Fig. 2B, Ima5p was much more active on panose than Ima1p (3.5-fold more activity whatsoever the panose concentration), but it was barely active on sucrose (10-fold lower activity than Ima1p) and was totally inactive on α-MG. Finally, as is shown in Table 3 and Fig. 2, Ima3p exhibited the most divergent enzymological properties as this enzyme was 5–10-fold less active on α-MG and isomaltose than Ima1p, and inactive on isomaltotriose and panose as well as on kojibiose, leucrose and other trisaccharides. Paradoxically, this protein was able to cleave substrates with α-1,3 bonds such as nigerose and exhibited its highest activity on sucrose when assayed at very high concentration (see Fig. 2A). However, due to low affinity for this sugar, the catalytic efficiency of Ima3p on sucrose was 2 and 4 times lower than on isomaltose and on palatinose, respectively (Table 3).

2.6. Maltose inhibition of yeast isomaltases

Yamamoto and coworkers reported that maltose act as a competitive inhibitor of Ima1p [13], which agreed with its ability to bind in the substrate-binding site [13,14]. This study was nevertheless carried out at concentrations of isomaltose (50–500 mM) that, according to our results, were inhibitory for Ima1p. We therefore reconsidered this analysis using lower, non-inhibitory concentrations of isomaltose as substrate (up to 50 mM) and also investigated maltose inhibition of Ima5p (Fig. 3). Classical, linear plots that complement one another [26], *i.e.* the plot of $1/v$ against I *vs.* the plot of S/v against I (Fig. S6), provided evidence for a bimodal behaviour of the inhibition type of Ima1p by maltose, which was function of the substrate concentration range. The non-linear fitting of our experimental data to the general mixed inhibition model, a general case that includes all of the common types of inhibition as asymptotic or special cases [26], clearly indicated a competitive inhibition at low substrate concentration (K_i of 257 mM, alpha $K_i \rightarrow \infty$) while it specified a uncompetitive inhibition at high substrate concentration ($K_i \rightarrow \infty$, alpha K_i of 274 mM) (Fig. 3). About Ima5p, our data revealed a different pattern of inhibition with nearly concurring lines in both plots (Fig. S6), which is characteristic of a mixed inhibition model. The non-linear fitting of the data comforted this conclusion (327 mM for K_i and 458 mM for K'_i, Fig. 3), and further underlined the strong non-competitive component of this inhibition as indicated by similar constants (equal constants in case of non-competitive inhibition). We finally tested whether acarbose, which is a potent inhibitor of yeast maltase [27], was also able to inhibit yeast isomaltases. Preliminary results on Ima1p showed that 5 and 20 mM acarbose led to *approx*. 80% and 40% residual activity in the presence of 50 mM isomaltose as substrate, indicating that yeast isomaltases are likely less sensitive to acarbose as compared to maltase enzymes [27].

3. Discussion

3.1. Substrate specificity and inhibition of yeast isomaltases

This work completed the biochemical and enzymological analysis that was carried out on the isomaltase isoenzyme 1 encoded by *S. cerevisiae IMA1* [5,13,14] and shed light on several discrepancies in published data on substrate utilization by this type of enzyme in yeast [8–12]. We confirmed the preference of the four Ima proteins for the α-1,6 disaccharides isomaltose and palatinose [6,15], and despite some activity on isomaltotriose, they were totally inactive on longer isomalto-oligosaccharides (IMOs). This result could be somehow explained from the 3D-structure analysis of GH13 alpha-amylase family [1], which indicates that the preference for short IMOs results from the pocket-like structure of the active site as it is observed in the *Bacillus cereus* α-1,6-glucosidase [28,29]. This structure is unable to dock long-chain substrates, contrary to the shallow groove structure more characteristic of the active site of polysaccharide endo-hydrolases such as the isoamylase [30].

Our enzymological analysis also indicated a significant activity of Ima proteins on sucrose, which was notably the best substrate of Ima3p at high concentration. This activity on sucrose was

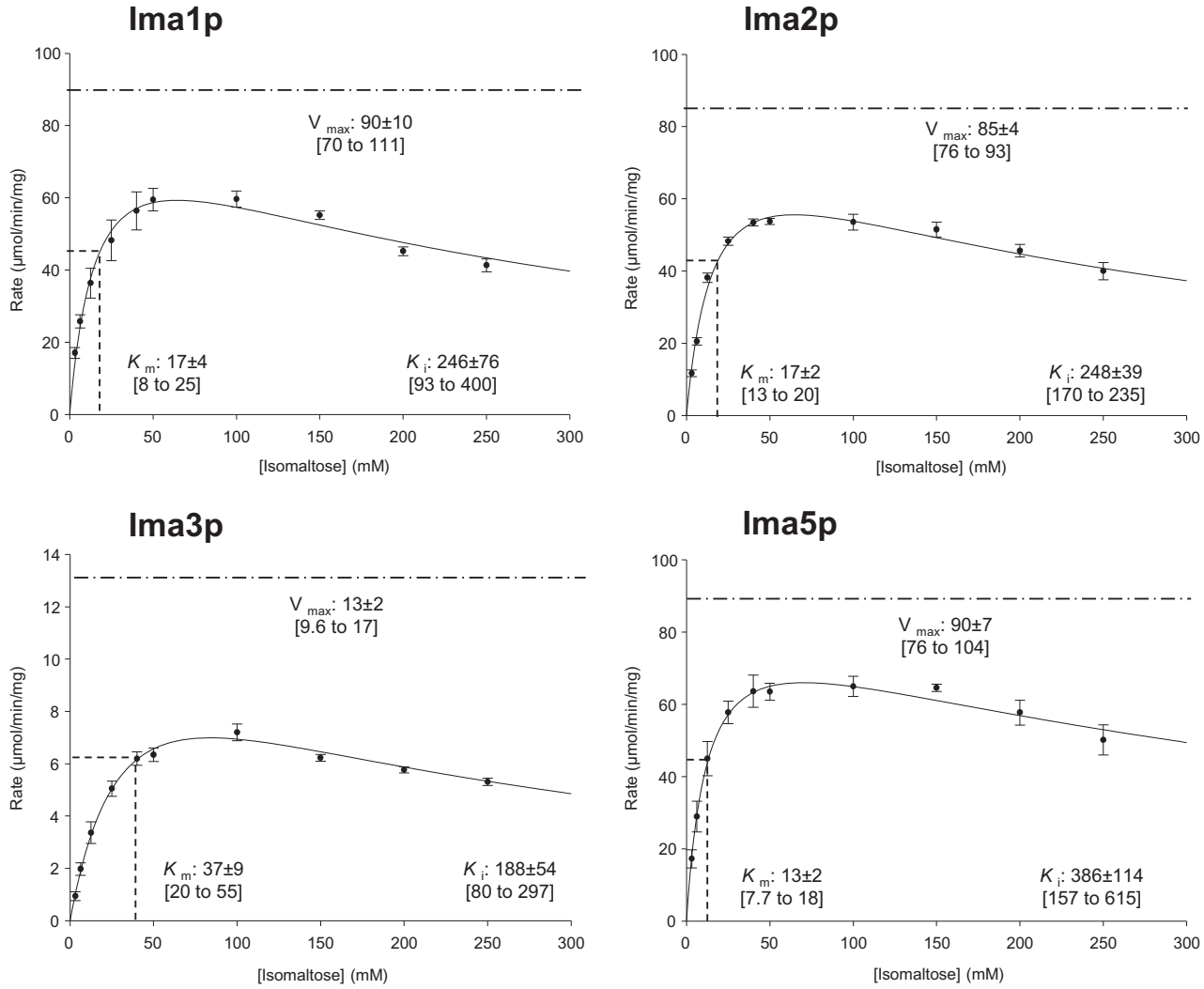

Fig. 1. Velocity–substrate profiles of Ima proteins for isomaltose. Non-linear curve fitting of the velocity as a function of substrate concentration, following the model $v = (V_{max}\,S)/(K_m + S(1 + S/K_i))$ with V_{max}: maximum velocity; S: substrate concentration; K_m: affinity constant and K_i: inhibition constant. Velocities were determined from an average of 5 independent assays. Estimated kinetic parameters, *i.e.* V_{max} (– · –), K_m (– – –) and K_i are expressed as the mean ± SEM. The 95% confidence interval is given between brackets.

contradictory reported in the literature [9,11], confirming the interest to biochemically analyse separately each isoenzyme. Khan and Eaton [9] most likely purified a mixture of Ima1p and Ima2p since their specific activity on sucrose was as high as for isomaltose. The so-called Glucosidase I isoenzyme purified by Matsusaka et al. [11], which was highly active on isomaltose yet hardly active on sucrose, could therefore look like the Ima5 isoform on these sole characteristics. But its specificities besides isomaltose and sucrose did not support this possibility and reinforce the existence of yet unknown and/or uncharacterized *IMA* encoded proteins in *S. cerevisiae* strains from various origins. Interesting variability in sucrose utilization by isomaltases also occurred in other yeast species, as the enzyme purified from the yeast *Torulaspora pretoriensis* presented the same activities on sucrose and isomaltose [16], while the yeast *Lipomyces starkeyi* α-glucosidase was totally inactive on sucrose [17]. Most α-1,4- and α-1,6-glucosidases from fungal kingdom [8,9,11,31–33] as well as α-glucosidases from honeybees [34] and *Bacillus* species [35,36] are also known to display sucrase activity with, however, most often lower k_{cat}/K_m than for their favoured substrate. We finally found that Ima proteins also cleaved the α-1,2 and α-1,3 glycosidic bonds of kojibiose, nigerose or turanose, similarly to what was observed for some broad substrate specificity α-glucosidases from honeybee [34], *Bifidobacterium breve* [37], *Bacillus* sp. SAM1606 [35] or *Bacillus thermoglucosidius* KP 1006 [38]. We can therefore conclude that yeast isomaltase isoenzymes exhibit multispecificity, also called substrate ambiguity, meaning that they are able to act on structurally related substrates [39,40].

As already pointed out in previous works [5–12], we confirmed that all Ima proteins were totally inactive on maltose. A very low specific activity on maltulose for Ima2p and Ima5p was nevertheless observed, which was comparable to the *B. breve* Alg1 and alg2 glucosidases [37]. Similarly, the yeast *T. pretoriensis* α-glucosidase exhibited 1% relative activity on maltose as compared to isomaltose [16]. It was therefore attractive to support the rule that an enzyme is able to cleave either isomaltose or maltose, not both. However, counterexamples could be found. We may cite the yeast *L. starkeyi* α-glucosidase that was indeed able to use maltose and isomaltose with high and similar efficiencies [17], as well as the honeybee *Apis mellifera* HBG-II protein [34,41–43]. These rare examples of proteins that developed activities towards both isomaltose and maltose with similar efficiencies therefore nuance to some extent the idea that both activities cannot be fully optimized in a single enzyme [8].

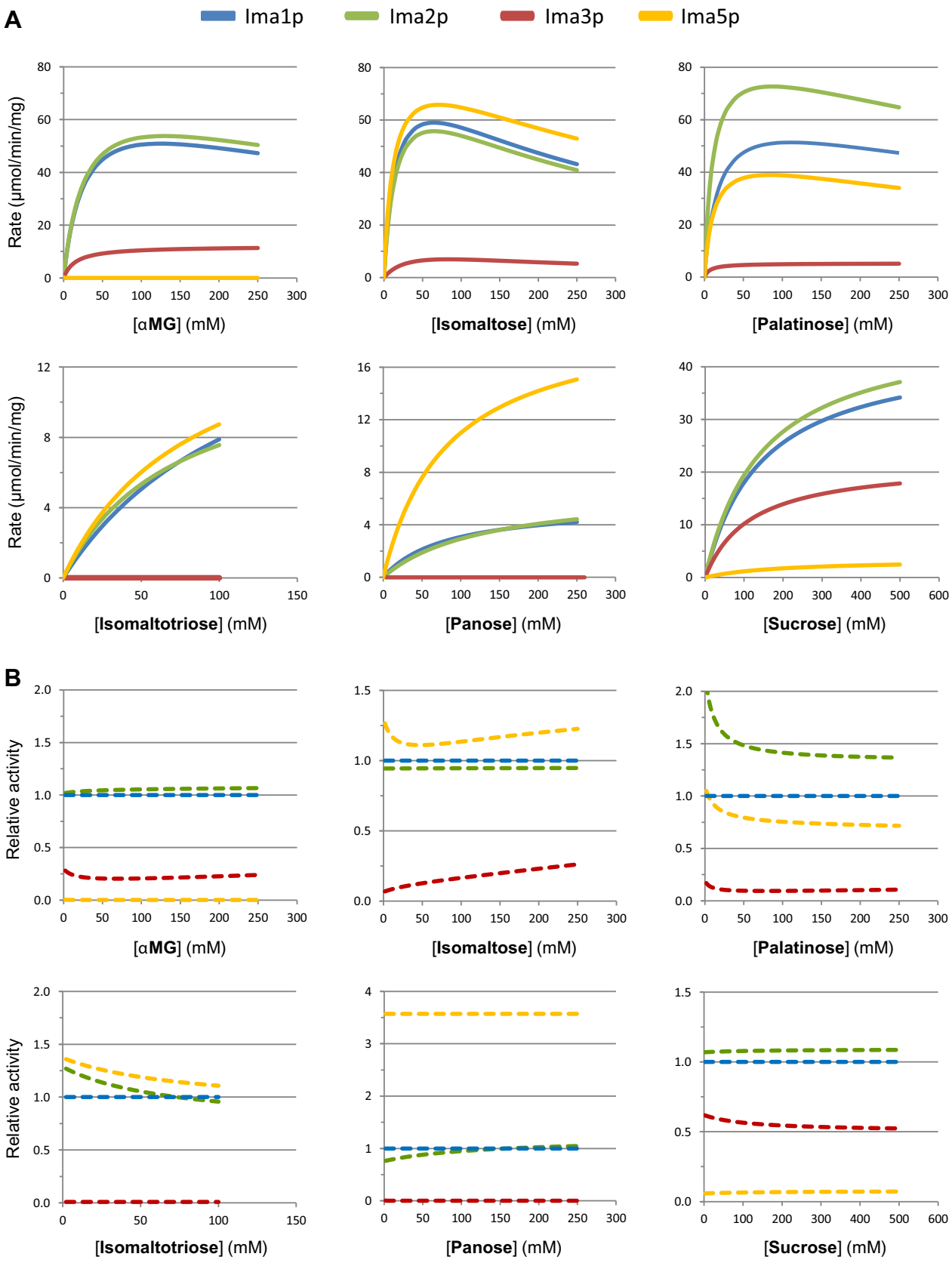

Fig. 2. Overview of Velocity-Substrate profiles and relative activities. Comparative plots of the four isomaltases (Ima1p, blue; Ima2p, green; Ima3p, red; Ima5p, yellow) on different substrates (α-MG, isomaltose, palatinose, isomaltotriose, panose and sucrose, respectively). (A) Representative curves of the velocity as a function of substrate concentration, plotted from the equation: $v = (V_{max}\,S)/(K_m + S(1 + S/K_i))$. For each isomaltase/substrate pair, V_{max}, K_m and K_i values can be found on the original plots (Fig. 1 and Fig. S4A–D). (B) Overview of relative activities, where the ratio of velocities (v_{Imaxp}/v_{Ima1p}, Ima1p being taken as the reference) is plotted as a function of substrate concentration. (For interpretation of the references to colour in this figure legend, the reader is referred to the web version of this article.)

Table 3
Kinetic parameters of Ima proteins for selected substrates.

Substrate	Ima1p				Ima2p			
	K_m (mM)	k_{cat} (s^{-1})	k_{cat}/K_m (mM^{-1} s^{-1})	K_i (mM)	K_m (mM)	k_{cat} (s^{-1})	k_{cat}/K_m (mM^{-1} s^{-1})	K_i (mM)
α-pNPG	0.58 ± 0.16	8.7 ± 1.0	15 ± 6	25 ± 15	0.89 ± 0.13	14 ± 1	16 ± 3	12 ± 3
α-MG	27 ± 5	84 ± 8	3.1 ± 0.9	574 ± 242	28 ± 6	88 ± 9	3.1 ± 1	600 ± 272
Isomaltose	17 ± 4	103 ± 12	5.7 ± 0.9	246 ± 76	17 ± 2	97 ± 5	5.6 ± 0.9	248 ± 39
Palatinose	18 ± 4	78 ± 8	4.3 ± 1.4	686 ± 351	11 ± 2	104 ± 6	9.4 ± 1.8	690 ± 231
Isomaltotriose	128 ± 35	21 ± 4	0.16 ± 0.07	None	72 ± 16	15 ± 2	0.21 ± 0.07	None
Panose	82 ± 17	6.3 ± 0.5	0.078 ± 0.023	None	129 ± 23	7.7 ± 0.7	0.051 ± 0.004	None
Sucrose	144 ± 26	51 ± 4	0.35 ± 0.09	None	147 ± 24	55 ± 4	0.38 ± 0.09	None
	Ima3p				Ima5p			
α-pNPG	0.35 ± 0.09	7.1 ± 0.7	20 ± 7	9.8 ± 3.2	0.48 ± 0.11	14 ± 1	28 ± 9	33 ± 21
α-MG	15 ± 2	14 ± 1	0.9 ± 0.1	None	0	0	0	None
Isomaltose	37 ± 9	15 ± 2	0.41 ± 0.15	188 ± 54	13 ± 2	101 ± 8	8.0 ± 2.2	386 ± 114
Palatinose	7.0 ± 0.7	6.0 ± 0.1	0.8 ± 0.1	None	12 ± 3	56 ± 5	5.0 ± 1.6	589 ± 266
Isomaltotriose	0	0	0	None	83 ± 25	18 ± 3	0.22 ± 0.10	None
Panose	0	0	0	None	82 ± 12	23 ± 1	0.28 ± 0.06	None
Sucrose	116 ± 12	25 ± 1	0.22 ± 0.03	None	191 ± 24	3.8 ± 0.2	0.020 ± 0.004	None

The affinity constant (K_m) and the catalytic constant (k_{cat}) were deduced from the curve of velocity as a function of substrate concentration and are expressed as the mean ± SEM. This table also indicates if an inhibition by high concentration of substrate was observed (K_i).

Maltose is not a substrate of yeast isomaltase, but it acts as an inhibitor of this enzyme. We showed in the present study that the inhibition was more complex than it was previously reported [13]. In the case of Ima1p, we found that the competitive inhibition was strictly restricted to very low substrate concentrations (up to *approx.* 10 mM), while it switched to the uncompetitive mode as the isomaltose concentration increased up to 50 mM, yet a non-inhibitory concentration of substrate. Very interestingly, Ima5p highlighted a different behaviour, with a mixed inhibition mode in the presence of maltose. Nevertheless, whatsoever the isomaltases and the mode of inhibition, estimates of K_i all fall in the range of several hundred mM. These values contrasted with K_i in the μM range that have been reported for potent inhibitors such as the acarbose and its derivative compounds, in the case of several α-glucosidases including yeast maltase [27,44]. The physiological relevance of the inhibition by maltose is therefore questionable.

3.2. Insights into structural determinants for substrates specificities

The existence of a crystal structure of Ima1p in complex with various substrates [13,14] together with the recent study by Voordeckers et al. [8] provided the first clues in the structural determinants for Ima1p activity, which can be extended to Ima2p and Ima3p due to their high sequence identity with Ima1p. Very interestingly, Ima2p and Ima3p properties markedly diverged from each other, although their amino acid sequence differed only by three amino acids. About substrates specificities and catalytic efficiency, the fundamental role of the residues Q279 and V216 for activity on α-1,6 bonds was very recently discussed and emphasized [8]. Accordingly, we observed that the replacement in Ima3p of the large, positively charged arginine residue by Q at position 279 resulted in a Ima3p_R279Q variant presenting kinetic properties similar to Ima2p. Careful analysis of Ima1p crystal structure indicated that Q279 and Y158 side chains are in interaction through an hydrogen bond (see Fig. 4, panels A and B). This interaction is likely not possible in Ima3p, which probably leads to the reorientation of R279 and/or Y158 side chains within the catalytic pocket and, as a consequence of this steric hindrance, to the observed loss of activity. However, the ability for Ima3p to cleave substrates with α-1,3 bonds as well as α-1,2 linkage of sucrose, suggested that the recognition and/or cleavage mechanism of these sugars can occur independently of the R and/or Q279 residue and therefore diverge from α-1,6 related substrates.

More phylogenetically distant, Ima5p displays *approx.* 65% sequence identity with the remaining members of the family. We then only focussed our attention on the consensus regions I to IV, with the replacement of the triplet VGI in Ima5p by MQH conserved in Ima1 and Ima2 proteins (position 278–280) (Fig. 4C and D). Surprisingly, this substitution led to a complete loss of activity of Ima5p, indicating that the full conservation of this consensus core cannot be assigned as the sole molecular basis of the enzymological properties of isomaltases. Other amino acids were identified in substrate binding or located near the binding pocket [8,13,14] and amongst them, amino acids at position 158, 219, 307 or 411 likely form a favourable environment for substrate recognition and cleavage [8]. Notably, the spatial cluster Q279-V216-L219 found in Ima1–4 proteins was described as important for substrate specificity of isomaltases, with the need for one protruding residue (Q279 in Ima1/2p) that leads to stabilization of isomaltose-like substrates while causing steric hindrance of the maltose-like sugars [8]. In the native Ima5p, the VGI triplet co-occurs with a methionine residue at position 219, therefore leading to the spatial vicinity of residues G279, V216 and M219 that somehow respects this need for only one protruding residue (see Fig. 4C). Also, Ima1p-based modelling of both Ima5 protein and of its Ima5p_MQH variant, using the Swiss-model tool [45] (see Sup. material), allowed us to notice that this protruding M219 probably co-evolved with a valine at position 177, instead of a leucine that might be incompatible with the M219 found in Ima5p. Similarly, we noticed that the tyrosine residue at position 158 was replaced by a phenylalanine in Ima5p, which, while keeping the huge phenyl ring on the side chain, does not lead to steric hindrance with G279 (Fig. 4C). Considering that the three dimensional organization of the active site of the Ima5p_MQH variant is identical to Ima1p or Ima5p, as is shown in Fig. 4D, it is incontestable that it leads to exacerbated steric hindrance in the catalytic pocket, arising in particular from (i) the simultaneous presence of two protruding amino acid residues surrounding V216, *i.e.* glutamine (Q279) and methionine (M219), and (ii) the lack of hydrogen bonding between Q279 and F158 in the absence of the hydroxyl group on the phenyl ring. We could therefore propose two alternatives for this variant. The first can be a reorientation *a minima* of these amino acids to minimize their interactions, which was not *de facto* anticipated by the homology modelling software due to the tightly packed environment of these side-chains. The second could be a more significant rearrangement in this region of the protein, with a local relocation of the backbone

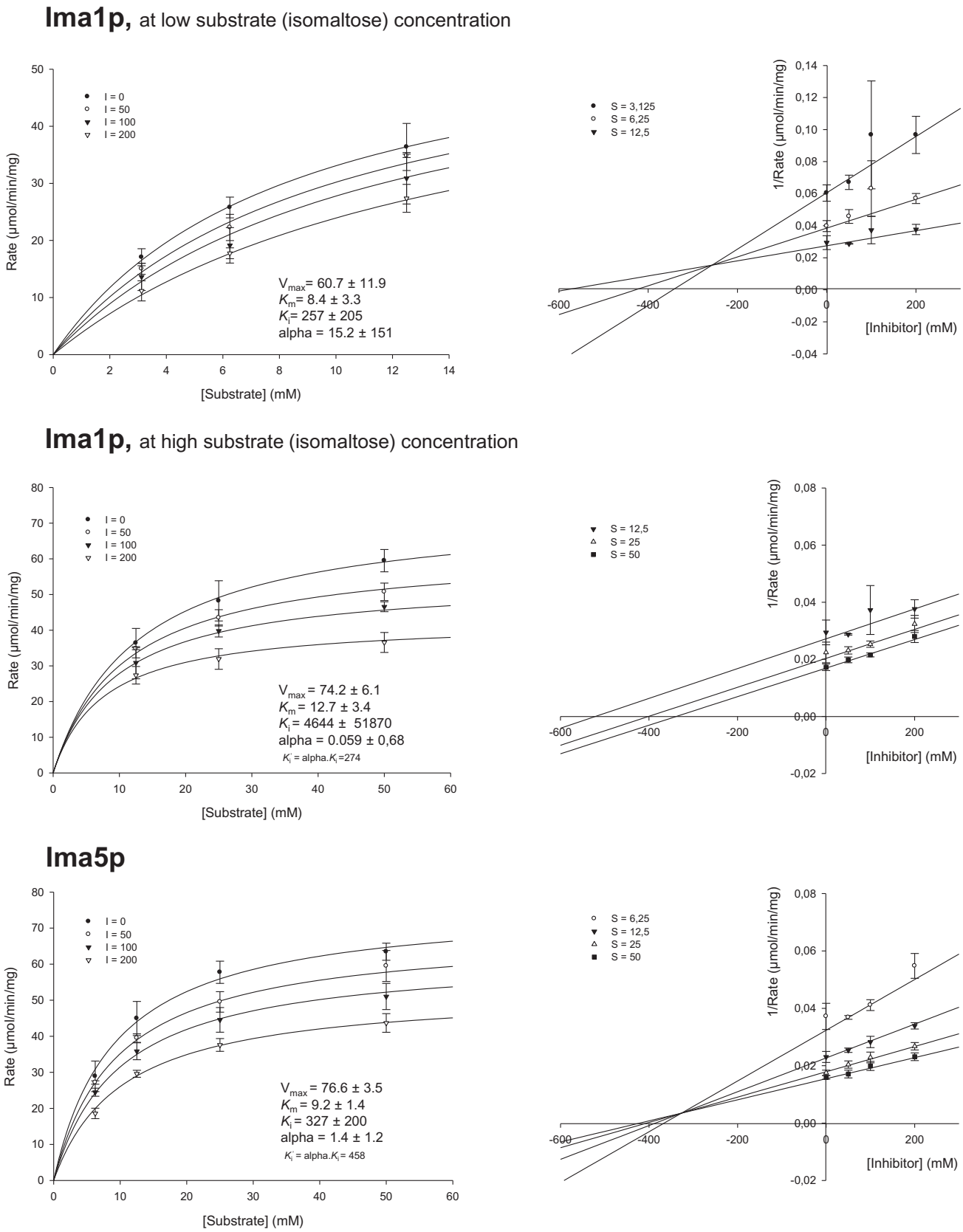

Fig. 3. Kinetic parameters of the inhibition by maltose. Left column (Michaëlis–Menten plots): Plot of velocity as a function of substrate (*i.e.* isomaltose) concentration in the absence (●) or in the presence of 50 mM (○), 100 mM (▼) or 200 mM (▽) inhibitor (*i.e.* maltose). Kinetic parameters were determined from non-linear curve fitting to the general, mixed inhibition model ($v = (V_{max}\ S)/[K_m(1 + I/K_i) + S(1 + I/K'_i)]$), performed by using the single substrate–single inhibitor inhibition option of the SigmaPlot Enzyme Kinetics 1.3 module. V_{max}: maximum velocity; S: substrate concentration; I: inhibitor concentration; K_m: affinity constant; K_i: inhibition constant and K'_i = alpha K_i. Results are from 3 independent assays. Estimated kinetic parameters are reported on the plots as the mean ± SEM. Right column (Dixon plots): Reciprocal of velocity as a function of inhibitor (*i.e.* maltose) concentration for substrate (isomaltose) concentrations of 3.125 mM (●), 6.25 mM (○), 12.5 mM (▼), 25 mM (△) or 50 mM (■). Inter-dependent lines drawn from the SigmaPlot Enzyme Kinetics module, using kinetic parameters from the non-linear curve fitting to the general, mixed model.

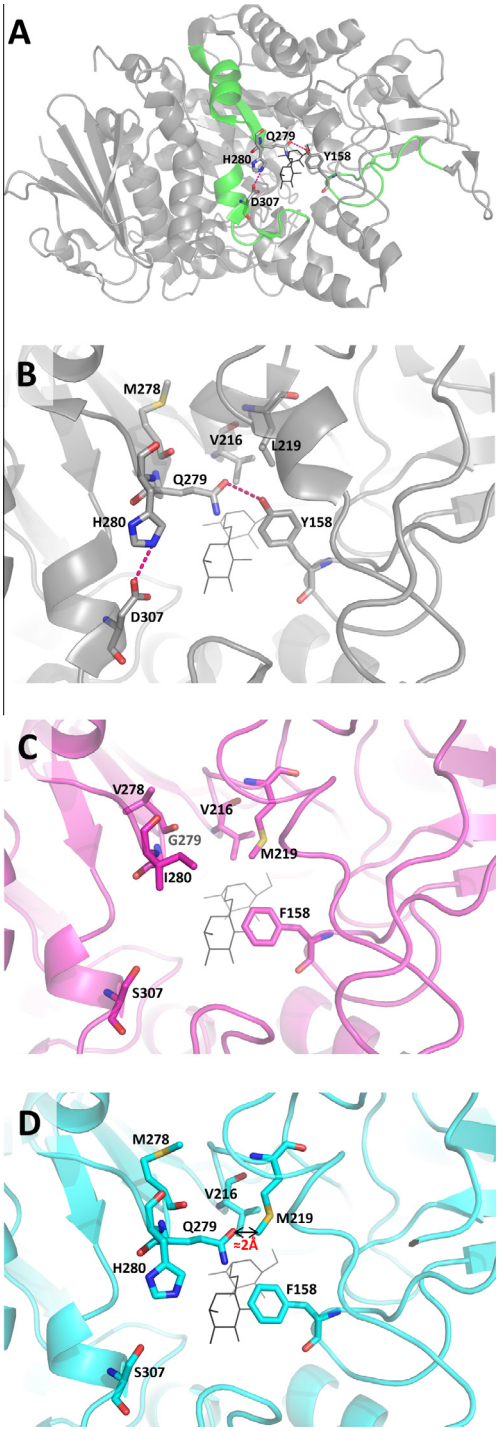

Fig. 4. Spatial organization of the active sites of Ima1p and Ima5p enzymes. Important amino acid residues discussed in this work were highlighted as sticks. (A) Global X-ray structure of Ima1p (pdb code: 3AJ7) showing isomaltose (black lines) in the active site pocket. The salt-bridge between H280 and D307 (red dashed line), probably helps maintaining the vicinity of the loops (residues 273–292 and 303–314 highlighted in green) and the thermal properties of Ima1p in a pH dependent manner. The positioning of the third, green loop (residues 150–164) is also probably important, keeping in interaction the side chains of Q279 and Y158 through an hydrogen bond (dashed line). Panel (B) shows details of the active site of Ima1p. Panel (C) shows a similar view of the Ima1p-based model of Ima5p protein (pdb file provided as Supplementary material). Panel (D) highlights the steric hindrance in the active site of Ima5p after replacement of VGI by MQH (pos. 278–280), which probably explains the total loss of activity in this protein variant. This figure was generated using Pymol (Delano Scientific, http://pymol.sourceforge.net/). (For interpretation of the references to colour in this figure legend, the reader is referred to the web version of this article.)

fundamentally different than what is shown. But in both case, the consequence is a dramatic collapse of the catalytic activity for this Ima5p_MQH variant, whatever the substrate.

More generally about catalytic activity within this protein family, the results obtained with Ima5p challenged previous conclusions that (i) the V216 and Q279 residues are largely responsible for determining the specificity of α-glucosidases for α-1,6 substrates and that (ii) the presence of Ala, Gly, or Asn residues at position 279 are considered as determinant for α-1,4-glycosidic hydrolyzing activity [14]. Here, we could show that Ima5p was fully active on α-1,6 substrates while bearing a glycine residue at position 279, and that the insertion of a Q at position 279 (VGI to MQH Ima5p variant) totally eliminated the activity of this protein. Finally, D307 was not identified as a catalytic residue in Ima1p [13] and its substitution by a serine in Ima5p further sustains that residue 307 is not important for the catalytic mechanism in Ima proteins.

3.3. Heterogeneous thermostability in the Ima protein family

Our study particularly underlined the low thermostability of the four yeast isomaltases that exhibited rather short half-life values and low melting temperatures. We observed that Tm values were significantly enhanced in the presence of Tris, a substrate-mimicking molecule which otherwise strongly inhibited these enzymes. This result could be consistent with the finding that a Tris molecule can bind the active site of GH13 enzymes such as amylosucrases [46–48] and interfere with flexibility in this critical region [49]. Strikingly and contrary to what might have been expected, the presence of maltose that was also found to bind the catalytic site [13] did not affect the melting temperature (results not shown). As another stabilizing factor, we suspected a role of calcium as an enhancer of the thermal stability of yeast isomaltases. Such a positive role was demonstrated for alpha-amylases [19] and for the *S. mutans* dextran glucosidase (SmDG, [20]), a GH13 enzyme that identically to Ima proteins, bears a calcium ion tightly bound to the first beta-alpha loop of the core barrel. Our results clearly indicated that the calcium ion has no effect on the thermostability of yeast isomaltases. The perfect conservation of the residues involved in calcium coordination therefore raised the question of its functional relevance for yeast isomaltases.

Ima1p and Ima2p shared identical thermal characteristics despite 39 different amino acids in their primary sequence. In contrast, Ima3p exhibited significant differences in thermal stability as compared to Ima2p while these two proteins differ by only three amino acids, including the Leu-to-Pro substitution at position 240 that appeared as an interesting target. Suzuki et al. indeed found a strong correlation between the increase in the number of proline residues and the rise in the thermostability of bacillary oligo-1,6 glucosidases [50]. Later, they have shown that cumulative replacements with proline residues could result in the additive enhancement in thermostability of oligo-1,6-glucosidase from *B. cereus* [29,51,52]. Other reports also showed that single proline substitution can be critical for thermostabilization [21–24]. In the present study, we found in agreement with these statements that the replacement of L240 by a Proline in Ima3p strongly enhanced the thermostability of this protein. However, since this L240P substitution did not allow full recovery of Ima2p characteristics, we can reasonably suggest that the replacement of the A54 residue by a threonine in the first beta-alpha loop of the core barrel of Ima3p participates in the lower thermostability of this protein. The polar and bulkier side-chain of T54, oriented within this core barrel, probably destabilizes this region of the macromolecular structure, accentuating Ima3p sensitivity to heat. Differences in key positions of proline residues in Ima5p might also explain the great

temperature sensitivity of this isoenzyme. Indeed, while the total number of proline residues in Ima1p and Ima5p is approximately the same (30 *vs*. 29, respectively), few of them are differentially located (Fig. S1). Interestingly, four amongst the six proline residues specific to Ima1p are located in the first N-terminus turn of alpha helices, which is recognized as a favourable position for helix stabilization, and one is found in a strict beta-turn, which also reinforces the rigidity of the loop. On the contrary, only one of the five residues specific to Ima5p is located in a beta turn, the four remaining residues being located outside these assigned structural features. Altogether, these observations support a positive role of these specific prolines for improved thermostability of Ima1p relative to Ima5p.

In addition to X-to-Pro substitutions, other relevant factors contribute to stability towards temperature of thermophilic enzymes, *e.g.* disulfide bridges, compactness of the hydrophobic core, intensification of surface salt-bridge networks, or alpha-helix dipole interactions as well as diverse residue substitutions [53]. Some of these elements probably apply to the Ima proteins and explain the differences between the most, Ima1p, and the least stable Ima5 protein. Ima5p contains 7 cysteine residues and 5 of them are conserved in Ima1p, but 3D-analysis of their relative positioning indicated that none of them could initiate disulfide-bridges. About the putative salt-bridge network that may differentiate these proteins, histidine-based salt-bridges are particularly relevant and may account for the huge impact of the pH on melting temperature of Ima1/2/3 proteins. Histidine is indeed the only residue whose pK_a of the side chain allows significant changes of electrical charge when increasing the pH value of the buffer from 6 to 8. The crystal structure of Ima1p revealed that residue H280 is salt-bridged to D307, but this salt-bridge does not exist in Ima5p due to the substitution of H280 and D307 by I and S, respectively (see Fig. 4). New formal X-ray structure, especially from the most divergent protein Ima5p and its MQH variant, will nevertheless be required to provide a firm foundation for comparative analysis and further insights into structural determinants for activity and thermostabilization mechanisms within this Ima protein family.

3.4. Conclusions

The presence of duplicated genes in a same species has a crucial role in evolutionary processes, especially in the rapid development of new functions [54,55]. The large 'Mal' multigene family from the yeast *S. cerevisiae* encompasses the *IMA* and related *MAL* subtelomeric genes. The fast expansion and evolution of these subtelomeric genes [7] motivated their use as a model system to provide experimental evidences on the mechanisms that allow such families to evolve from a common promiscuous ancestor [8]. While addressing the clear-cut difference between the α-1,4 and α-1,6 specificities in this large 'Mal' family, these authors proposed that gene duplications repeatedly spawned daughter genes in which mutations optimized the subfunctions separately in different paralogs, to circumvent adaptive constraints on a multifunctional gene [8]. However, quantitative data reported in the present work showed that besides the α-1,6 glycosidase activity, relevant activities on sucrose or α-1,3 disaccharides still persisted to different extent in the Ima protein family. This substrate 'ambiguity' probably enhances the phenotypic plasticity required for sugar utilization in microorganisms such as the yeast *S. cerevisiae*.

Our in-deep biochemical analysis of this Ima protein family also illustrated evolutionary singularities, highlighting how mutations on a few key amino acids residues can lead to significant biophysical and enzymological effects. For instance, the recent duplication events within the family indeed led to two identical genes, *IMA3* and *IMA4* that encode a protein with only 3 different amino acids with Ima2p, but these proteins present significant differences in both catalytic characteristics and thermostability. Also, while being the most phylogenetically divergent protein within this family, Ima5p exhibited highly altered thermostability but displayed most of Ima1p and Ima2p catalytic properties. This later result supported Voordeckers et al. idea [8] that different evolutionary routes leading to variable amino acids combinations can result in similar changes in substrate specificities, and also highlights the robustness of biological systems through evolution.

4. Experimental procedures

4.1. Chemicals and biochemical reagents

α-pNPG (N1377), β-pNPG (N7006), maltose (M5885), sucrose (S0389) and α-MG (M9376) were purchased from Sigma-Aldrich. Isomaltose (MI04560), palatinose (OI04225), isomaltotriose (OI05352), panose (OP06685), trehalose (OT03932), kojibiose (OK05039), nigerose (ON06975), turanose (OT06692), maltulose (OM06578), leucrose (OL06727), maltotriose (OM06486) and melezitose (OM00386) were purchased from Carbosynth. These sugars were chosen with the highest purity as possible and were further analysed by HPAE-PAD (Dionex ICS3000 system equipped with a carbopac PA10 analytical ion exchange column and pulsed amperometric detector) to confirm their purity. All other chemicals were purchased from Sigma. Glucose-6-phosphate dehydrogenase (101276550001) and hexokinase (11426362001) were purchased from Roche Diagnostics.

4.2. Cloning, expression and purification of proteins

The *IMAx* sequences encoding isomaltases from *S. cerevisiae* (*IMA1*/*YGR287C*, *IMA2*/*YOL157C*, *IMA3*/*YIL172C*, *IMA5*/*YJL216C*) were amplified by PCR using the pGEMt-IMAx plasmids as template [6] (primers listed in Table S1). The coding sequences were cloned in the pYES2.1 TOPO® TA vector (Life Technologies), allowing expression in yeast of the protein with a polyhistidine tag at the C-terminus. DNA fragments bearing mutations leading to the expression of Ima3_L240P (CGAAAA**TTC**AAAGTGGCAACCCAGTG; CTC→**TTC**: L240P mutation; Underlined: silent mutation, *Dde*I lost), Ima3_R279Q (GAAATG**CAA**CACGCTACT; GAC→**CAA**: R279Q mutation; Underlined: silent mutation, *Nsp*I lost) and Ima5_VGI-MQH (TTCCCGAGGGT(N)$_{21}$GAA**ATGCAGCAC**GGA; GTTGGTATC→**ATGCAGCAC**: VGI to MQH mutation; Underlined: silent mutation, *Ava*I added) variants were synthesized by Eurofins MWG Operon (Ebersberg, Germany). *Mfe*I mutated fragments of *IMA3* (854 bp) were inserted into *Mfe*I sites of the pYES2.1 TOPO/IMA3 plasmid yielding to the final expression vectors. Similarly, the *Tth111*I/*Sal*I mutated fragment of *IMA5* (896 bp) was subcloned into the pYES2.1 TOPO/IMA5 plasmid. All plasmids were verified by sequencing.

Transformation of the yeast strain CEN.PK113-5D (MATa *ura3-52 MAL2-8^c SUC2*) [56,57] was performed according to the lithium acetate method [58]. To induce the expression of the protein, cells were grown in YN medium (0.17% yeast nitrogen base without amino acid and without ammonium, 0.5% ammonium sulphate) in the presence of 2% raffinose (w/v) at 30 °C overnight (OD_{600} *approx.* 4), and then diluted to OD_{600} 0.4 in YN medium in the presence of 2% galactose for 6 h. 50 mL of growing cells, enough to get *approx.* 30 μg of purified protein, were collected by centrifugation (2000*g*, 5 min), washed with 1 mL of water and frozen at −20 °C before use. Crude extract containing recombinant His-tagged proteins was prepared extemporaneously from an adequate number of pellets as described previously [6], except that the extraction buffer contained 50 mM potassium phosphate buffer pH 7 and

1 mM PMSF. After initial washing of the TALON® Metal Affinity Resin (Clontech, Ref. 635503), crude extracts from two pellets were pooled and mixed to 150 μL bed volume of this equilibrated resin with gentle agitation at room temperature for 35 min. Two successive washes with 625 μL of 1× Equilibration/Wash Buffer were performed with gentle agitation at room temperature for 10 min. The bound protein was released from the affinity resin with three successive elutions, *i.e.* 125 μL of 1× Equilibration/Wash Buffer containing 150 mM imidazole, then 75 μL in the presence of 260 mM imidazole and finally with 75 μL containing 350 mM imidazole. Protein purity was examined on SDS/PAGE after Coomassie Blue staining. Protein concentration was determined by the Bradford assay (Bio-Rad protein assay dye reagent, Ref. 500-0006) using BSA as protein standard.

4.3. Enzyme assays

Unless otherwise stated, the enzyme assays were carried out at 30 °C, pH 7, in 1 mL reaction mix containing 500 μL of citrate–potassium phosphate buffer. Reactions were followed continuously by using the thermo-stated Agilent 8453 spectrophotometer. The α-glucosidase activity was assayed by using α-*p*-nitrophenyl-D-glucopyranoside (α-pNPG) as substrate [59] and monitoring the release of *p*-nitrophenyl (pNP) at 405 nm. Activity on the other substrates, including the α-MG, was measured by using a coupled spectrophotometric assay between the release of glucose and the production of NADPH at 340 nm, with the simultaneous use in the assay of hexokinase and glucose-6-phosphate dehydrogenase. The reaction was started by the addition of 20 μL freshly purified protein to the 1 mL reaction mix containing 5 mM $MgCl_2$, 1 mM ATP, 1 mM NADP, 5 units of hexokinase, 5 units of glucose-6-phosphate dehydrogenase and substrate at desired final concentration. Velocities were determined as the initial reaction rates (v), which were proportional to the amount of purified protein added.

4.4. Determination of biochemical parameters

The pH profile was determined at 30 °C in the citrate–potassium phosphate buffer (pH 2.6–8) and in the potassium phosphate buffer (pH 7–9), while the temperature profile was characterized at pH 7 and at temperatures ranging from 20 to 60 °C, using pNPG at 5 mM as the substrate. For thermostability assays, the activity was followed over time by setting the reaction at a given temperature (37, 40 or 42 °C) and the half-life ($t_{1/2}$) was determined from the derivative of the curve of pNP production as a function of time. This derivative curve was fitted using the exponential equation: $v(t) = v\,e^{-\lambda t}$, with λ the decay constant ($\lambda = \mathrm{Ln}2/t_{1/2}$), v the initial reaction rate and $v(t)$ the residual velocity at time t. The melting temperature (T_m) of isomaltases was assayed by differential scanning fluorimetry (DSF). A mixture of enzyme (5 μM), Sypro-orange (5×) (Invitrogen, S6650), and citrate–potassium phosphate buffer, pH 7, were incubated with an increase of temperature from 25 to 80 °C (0.3 °C increment every 0.3 s). The fluorescence was monitored by using the CFX96 Real-time System (Bio-Rad). The thermal transition (T_m) corresponds to the inflection point of the transition curve (fluorescence unit = $f(T)$) and was calculated as the maximum of the first derivative.

4.5. Determination of kinetic parameters

Kinetic parameters were calculated from substrate concentrations ranging from 0.39 to 10 mM for pNPG, from 3.125 to 250 mM for palatinose, isomaltose and α-MG, from 3.125 to 100 mM for isomaltotriose, from 12.5 to 200 mM for panose and from 15.625 to 500 mM for sucrose. V_{max}, K_m and K_i (when substrate inhibition occurred) were computed by non-linear curve fitting of the velocity as a function of substrate concentration (Figs. S4A–D and S5), using the Enzyme Kinetics 1.3 module of the SigmaPlot 11.0 package (Systat Software, IL, USA). The catalytic constant k_{cat} of the enzyme was calculated from $k_{cat} = V_{max}/[E]$. The molar concentration [E] was 68.6 kDa for Ima1p and Ima2p, 68.7 kDa for Ima3p and 67.6 kDa for Ima5p. Maltose inhibition was analysed with isomaltose (substrate) concentrations below 50 mM to avoid substrate inhibition. Kinetic parameters, including inhibition constants, were calculated by non-linear curve fitting by using the 'single substrate–single inhibitor' model of the SigmaPlot Enzyme Kinetics module.

4.6. Statistical analysis

The results reported in this work were from an average of 5 experiments, carried out on independent and extemporaneous enzyme preparations. Estimates of kinetic parameters through non-linear curve fitting (K_m, k_{cat}, K_i, V_{max}) and associated statistical data (*e.g.* standard errors (SEM), confidence intervals or predicted values) were directly provided by the SigmaPlot Enzyme Kinetics module. The statistical tests on half-life and DSF values (Table 1) or on the velocities in presence of putative effectors (Fig. S2), were performed by using the STATGRAPHICS Centurion 16 software.

4.7. Homology modelling and multiple sequence alignment

The fully automated protein structure homology-modelling server Swiss Model [60,61] was used for homology modelling of Ima5p protein structure. Modelling was carried out by the automated mode and the generated model was displayed and compared with the crystal structure of Ima1p (PDB: 3AJ7) using coot software [62]. The multiple sequence and structural alignment was generated with ESPript [63].

Acknowledgements

Xu Deng held a Ph.D. grant from the China Scholarship Council. We are grateful to Pr. Didier Combes and Dr. Gustavo De Billerbeck for their help and constructive advices. We also thank Amelie Vax for her help with sugar analysis using HPLC-Dionex and the IBiSA Integrated Screening Platform of Toulouse (PICT, IPBS, CNRS – Université de Toulouse) for providing access to DSF equipment.

Appendix A. Supplementary data

Supplementary data associated with this article can be found, in the online version, at http://dx.doi.org/10.1016/j.fob.2014.02.004.

References

[1] MacGregor, E.A., Janecek, S. and Svensson, B. (2001) Relationship of sequence and structure to specificity in the alpha-amylase family of enzymes. Biochim. Biophys. Acta 1546, 1–20.
[2] Stam, M.R., Danchin, E.G., Rancurel, C., Coutinho, P.M. and Henrissat, B. (2006) Dividing the large glycoside hydrolase family 13 into subfamilies: towards improved functional annotations of alpha-amylase-related proteins. Protein Eng. Sel. 19, 555–562.
[3] Cantarel, B.L., Coutinho, P.M., Rancurel, C., Bernard, T., Lombard, V. and Henrissat, B. (2009) The Carbohydrate-Active EnZymes database (CAZy): an expert resource for Glycogenomics. Nucleic Acids Res. 37, D233–D238.
[4] Saburi, W., Mori, H., Saito, S., Okuyama, M. and Kimura, A. (2006) Structural elements in dextran glucosidase responsible for high specificity to long chain substrate. Biochim. Biophys. Acta 1764, 688–698.

[5] Yamamoto, K., Nakayama, A., Yamamoto, Y. and Tabata, S. (2004) Val216 decides the substrate specificity of alpha-glucosidase in *Saccharomyces cerevisiae*. Eur. J. Biochem. 271, 3414–3420.
[6] Teste, M.A., Francois, J.M. and Parrou, J.L. (2010) Characterization of a new multigene family encoding isomaltases in the yeast *Saccharomyces cerevisiae*, the *IMA* family. J. Biol. Chem. 285, 26815–26824.
[7] Brown, C.A., Murray, A.W. and Verstrepen, K.J. (2010) Rapid expansion and functional divergence of subtelomeric gene families in yeasts. Curr. Biol. 20, 895–903.
[8] Voordeckers, K., Brown, C.A., Vanneste, K., van der Zande, E., Voet, A., Maere, S. and Verstrepen, K.J. (2012) Reconstruction of ancestral metabolic enzymes reveals molecular mechanisms underlying evolutionary innovation through gene duplication. PLoS Biol. 10, e1001446.
[9] Khan, N.A. and Eaton, N.R. (1967) Purification and characterization of maltase and alpha-methyl glucosidase from yeast. Biochim. Biophys. Acta 146, 173–180.
[10] Frandsen, T.P., Palcic, M.M. and Svensson, B. (2002) Substrate recognition by three family 13 yeast alpha-glucosidases. Eur. J. Biochem. 269, 728–734.
[11] Matsusaka, K., Chiba, S. and Shimomura, T. (1977) Purification and substrate specificity of Brewer's yeast alpha-glucosidase. Agric. Biol. Chem. 41, 1917–1923.
[12] Yoshikawa, K., Yamamoto, K. and Okada, S. (1994) Classification of some alpha-glucosidases and alpha-xylosidases on the basis of substrate specificity. Biosci. Biotechnol. Biochem. 58, 1392–1398.
[13] Yamamoto, K., Miyake, H., Kusunoki, M. and Osaki, S. (2010) Crystal structures of isomaltase from *Saccharomyces cerevisiae* and in complex with its competitive inhibitor maltose. FEBS J. 277, 4205–4214.
[14] Yamamoto, K., Miyake, H., Kusunoki, M. and Osaki, S. (2011) Steric hindrance by 2 amino acid residues determines the substrate specificity of isomaltase from *Saccharomyces cerevisiae*. J. Biosci. Bioeng. 112, 545–550.
[15] Naumoff, D.G. and Naumov, G.I. (2010) Discovery of a novel family of alpha-glucosidase *IMA* genes in yeast *Saccharomyces cerevisiae*. Dokl. Biochem. Biophys. 432, 114–116.
[16] Oda, Y., Iwamoto, H., Hiromi, K. and Tonomura, K. (1993) Purification and characterization of alpha-glucosidase from *Torulaspora pretoriensis* YK-1. Biosci. Biotechnol. Biochem. 57, 1902–1905.
[17] Kelly, C.T., Moriarty, M.E. and Fogarty, W.M. (1985) Thermostable extracellular alpha-amylase and alpha-glucosidase of *Lipomyces starkeyi*. Appl. Microbiol. Biotechnol. 22, 352–358.
[18] Orij, R., Brul, S. and Smits, G.J. (2011) Intracellular pH is a tightly controlled signal in yeast. Biochim. Biophys. Acta 1810, 933–944.
[19] Vallee, B.L., Stein, E.A., Sumerwell, W.N. and Fischer, E.H. (1959) Metal content of alpha-amylases of various origins. J. Biol. Chem. 234, 2901–2905.
[20] Kobayashi, M., Hondoh, H., Mori, H., Saburi, W., Okuyama, M. and Kimura, A. (2011) Calcium ion-dependent increase in thermostability of dextran glucosidase from *Streptococcus mutans*. Biosci. Biotechnol. Biochem. 75, 1557–1563.
[21] Herning, T., Yutani, K., Inaka, K., Kuroki, R., Matsushima, M. and Kikuchi, M. (1992) Role of proline residues in human lysozyme stability: a scanning calorimetric study combined with X-ray structure analysis of proline mutants. Biochemistry (Mosc.) 31, 7077–7085.
[22] Li, Y., Reilly, P.J. and Ford, C. (1997) Effect of introducing proline residues on the stability of *Aspergillus awamori*. Protein Eng. 10, 1199–1204.
[23] Muslin, E.H., Clark, S.E. and Henson, C.A. (2002) The effect of proline insertions on the thermostability of a barley alpha-glucosidase. Protein Eng. 15, 29–33.
[24] Zhou, C., Xue, Y. and Ma, Y. (2010) Enhancing the thermostability of alpha-glucosidase from *Thermoanaerobacter tengcongensis* MB4 by single proline substitution. J. Biosci. Bioeng. 110, 12–17.
[25] Eisenthal, R., Danson, M.J. and Hough, D.W. (2007) Catalytic efficiency and kcat/KM: a useful comparator? Trends Biotechnol. 25, 247–249.
[26] Cornish-Bowden, A. (1974) A simple graphical method for determining the inhibition constants of mixed, uncompetitive and non-competitive inhibitors. Biochem. J. 137, 143–144.
[27] Kim, M.J., Lee, S.B., Lee, H.S., Lee, S.Y., Baek, J.S., Kim, D., Moon, T.W., Robyt, J.F. and Park, K.H. (1999) Comparative study of the inhibition of alpha-glucosidase, alpha-amylase, and cyclomaltodextrin glucanosyltransferase by acarbose, isoacarbose, and acarviosine-glucose. Arch. Biochem. Biophys. 371, 277–283.
[28] Kizaki, H., Hata, Y., Watanabe, K., Katsube, Y. and Suzuki, Y. (1993) Polypeptide folding of *Bacillus cereus* ATCC7064 oligo-1,6-glucosidase revealed by 3.0 A resolution X-ray analysis. J. Biochem. 113, 646–649.
[29] Watanabe, K., Hata, Y., Kizaki, H., Katsube, Y. and Suzuki, Y. (1997) The refined crystal structure of *Bacillus cereus* oligo-1,6-glucosidase at 2.0 A resolution: structural characterization of proline-substitution sites for protein thermostabilization. J. Mol. Biol. 269, 142–153.
[30] Katsuya, Y., Mezaki, Y., Kubota, M. and Matsuura, Y. (1998) Three-dimensional structure of *Pseudomonas* isoamylase at 2.2 A resolution. J. Mol. Biol. 281, 885–897.
[31] Krakenaite, R.P. and Glemzha, A.A. (1983) Some properties of two forms of alpha-glucosidase from *Saccharomyces cerevisiae*-II. Biokhimiia 48, 62–68.
[32] Geber, A., Williamson, P.R., Rex, J.H., Sweeney, E.C. and Bennett, J.E. (1992) Cloning and characterization of a *Candida albicans* maltase gene involved in sucrose utilization. J. Bacteriol. 174, 6992–6996.
[33] Williamson, P.R., Huber, M.A. and Bennett, J.E. (1993) Role of maltase in the utilization of sucrose by *Candida albicans*. Biochem. J. 291 (Pt 3), 765–771.
[34] Ngiwsara, L., Iwai, G., Tagami, T., Sato, N., Nakai, H., Okuyama, M., Mori, H. and Kimura, A. (2012) Amino acids in conserved region II are crucial to substrate specificity, reaction velocity, and regioselectivity in the transglucosylation of honeybee GH-13 alpha-glucosidases. Biosci. Biotechnol. Biochem. 76, 1967–1974.
[35] Noguchi, A., Yano, M., Ohshima, Y., Hemmi, H., Inohara-Ochiai, M., Okada, M., Min, K.S., Nakayama, T. and Nishino, T. (2003) Deciphering the molecular basis of the broad substrate specificity of alpha-glucosidase from *Bacillus* sp. SAM1606. J. Biochem. 134, 543–550.
[36] Schonert, S., Buder, T. and Dahl, M.K. (1998) Identification and enzymatic characterization of the maltose-inducible alpha-glucosidase MalL (sucrase–isomaltase–maltase) of *Bacillus subtilis*. J. Bacteriol. 180, 2574–2578.
[37] Pokusaeva, K., O'Connell-Motherway, M., Zomer, A., Fitzgerald, G.F. and van Sinderen, D. (2009) Characterization of two novel alpha-glucosidases from *Bifidobacterium breve* UCC2003. Appl. Environ. Microbiol. 75, 1135–1143.
[38] Suzuki, Y., Ueda, Y., Nakamura, N. and Abe, S. (1979) Hydrolysis of low molecular weight isomaltosaccharides by a *p*-nitrophenyl-alpha-D-glucopyranoside-hydrolyzing alpha-glucosidase from a thermophile, *Bacillus thermoglucosidius* KP 1006. Biochim. Biophys. Acta 566, 62–66.
[39] Peric-Hassler, L., Hansen, H.S., Baron, R. and Hunenberger, P.H. (2010) Conformational properties of glucose-based disaccharides investigated using molecular dynamics simulations with local elevation umbrella sampling. Carbohydr. Res. 345, 1781–1801.
[40] Khersonsky, O. and Tawfik, D.S. (2010) Enzyme promiscuity: a mechanistic and evolutionary perspective. Annu. Rev. Biochem. 79, 471–505.
[41] Kimura, A., Takewaki, S., Matsui, H., Kubota, M. and Chiba, S. (1990) Allosteric properties, substrate specificity, and subsite affinities of honeybee alpha-glucosidase I. J. Biochem. 107, 762–768.
[42] Nishimoto, M., Kubota, M., Tsuji, M., Mori, H., Kimura, A., Matsui, H. and Chiba, S. (2001) Purification and substrate specificity of honeybee, *Apis mellifera* L., alpha-glucosidase III. Biosci. Biotechnol. Biochem. 65, 1610–1616.
[43] Takewaki, S., Kimura, A., Kubota, M. and Chiba, S. (1993) Substrate specificity and subsite affinities of honeybee alpha-glucosidase II. Biosci. Biotechnol. Biochem. 57, 1508–1513.
[44] Kimura, A., Lee, J.H., Lee, I.S., Lee, H.S., Park, K.H., Chiba, S. and Kim, D. (2004) Two potent competitive inhibitors discriminating alpha-glucosidase family I from family II. Carbohydr. Res. 339, 1035–1040.
[45] Arnold, K., Bordoli, L., Kopp, J. and Schwede, T. (2006) The SWISS-MODEL workspace: a web-based environment for protein structure homology modelling. Bioinformatics 22, 195–201.
[46] Skov, L.K., Mirza, O., Henriksen, A., De Montalk, G.P., Remaud-Simeon, M., Sarçabal, P., Willemot, R.M., Monsan, P. and Gajhede, M. (2001) Amylosucrase, a glucan-synthesizing enzyme from the alpha-amylase family. J. Biol. Chem. 276, 25273–25278.
[47] Guérin, F., Barbe, S., Pizzut-Serin, S., Potocki-Véronèse, G., Guieysse, D., Guillet, V., Monsan, P., Mourey, L., Remaud-Siméon, M., André, I. and Tranier, S. (2012) Structural investigation of the thermostability and product specificity of amylosucrase from the bacterium *Deinococcus geothermalis*. J. Biol. Chem. 287, 6642–6654.
[48] Champion, E., Guérin, F., Moulis, C., Barbe, S., Tran, T.H., Morel, S., Descroix, K., Monsan, P., Mourey, L., Mulard, L.A., Tranier, S., Remaud-Siméon, M. and André, I. (2012) Applying pairwise combinations of amino acid mutations for sorting out highly efficient glucosylation tools for chemo-enzymatic synthesis of bacterial oligosaccharides. J. Am. Chem. Soc. 134, 18677–18688.
[49] Skov, L.K., Pizzut-Serin, S., Remaud-Simeon, M., Ernst, H.A., Gajhede, M. and Mirza, O. (2013) The structure of amylosucrase from *Deinococcus radiodurans* has an unusual open active-site topology. Acta Crystallogr. Sect. F Struct. Biol. Cryst. Commun. 69, 973–978.
[50] Suzuki, Y., Oishi, K., Nakano, H. and Nagayama, T. (1987) A strong correlation between the increase in number of proline residues and the rise in thermostability of five *Bacillus* oligo-1,6 glucosidase. Appl. Microbiol. Biotechnol. 26, 546–551.
[51] Watanabe, K. and Suzuki, Y. (1998) Protein thermostabilization by proline substitutions. J. Mol. Catal. B Enzym. 4, 167–180.
[52] Watanabe, K., Masuda, T., Ohashi, H., Mihara, H. and Suzuki, Y. (1994) Multiple proline substitutions cumulatively thermostabilize *Bacillus cereus* ATCC7064 oligo-1,6-glucosidase. Irrefragable proof supporting the proline rule. Eur. J. Biochem. 226, 277–283.
[53] Lehmann, M., Pasamontes, L., Lassen, S.F. and Wyss, M. (2000) The consensus concept for thermostability engineering of proteins. Biochim. Biophys. Acta 1543, 408–415.
[54] Conant, G.C. and Wolfe, K.H. (2008) Turning a hobby into a job: how duplicated genes find new functions. Nat. Rev. Genet. 9, 938–950.
[55] Innan, H. and Kondrashov, F. (2010) The evolution of gene duplications: classifying and distinguishing between models. Nat. Rev. Genet. 11, 97–108.
[56] Nijkamp, J.F., van den Broek, M., Datema, E., de Kok, S., Bosman, L., Luttik, M.A., Daran-Lapujade, P., Vongsangnak, W., Nielsen, J., Heijne, W.H., Klaassen, P., Paddon, C.J., Platt, D., Kotter, P., van Ham, R.C., Reinders, M.J., Pronk, J.T., de Ridder, D. and Daran, J.M. (2012) De novo sequencing, assembly and analysis of the genome of the laboratory strain *Saccharomyces cerevisiae* CEN.PK113-7D, a model for modern industrial biotechnology. Microb. Cell Fact. 11, 36.
[57] Van Dijken, J.P., Bauer, J., Brambilla, L., Duboc, P., Francois, J.M., Gancedo, C., Giuseppin, M.L., Heijnen, J.J., Hoare, M., Lange, H.C., Madden, E.A., Niederberger, P., Nielsen, J., Parrou, J.L., Petit, T., Porro, D., Reuss, M., van Riel, N., Rizzi, M., Steensma, H.Y., Verrips, C.T., Vindelov, J. and Pronk, J.T.

(2000) An interlaboratory comparison of physiological and genetic properties of four *Saccharomyces cerevisiae* strains. Enzyme Microb. Technol. 26, 706–714.
[58] Gietz, R.D. and Schiestl, R.H. (2007) High-efficiency yeast transformation using the LiAc/SS carrier DNA/PEG method. Nat. Protoc. 2, 31–34.
[59] Dubin, R.A., Needleman, R.B., Gossett, D. and Michels, C.A. (1985) Identification of the structural gene encoding maltase within the *MAL6* locus of *Saccharomyces carlsbergensis*. J. Bacteriol. 164, 605–610.
[60] Schwede, T., Kopp, J., Guex, N. and Peitsch, M.C. (2003) SWISS-MODEL: an automated protein homology-modeling server. Nucleic Acids Res. 31, 3381–3385.
[61] Goujon, M., McWilliam, H., Li, W., Valentin, F., Squizzato, S., Paern, J. and Lopez, R. (2010) A new bioinformatics analysis tools framework at EMBL-EBI. Nucleic Acids Res. 38, W695–W699.
[62] Emsley, P. and Cowtan, K. (2004) Coot: model-building tools for molecular graphics. Acta Crystallogr. D Biol. Crystallogr. 60, 2126–2132.
[63] Gouet, P., Robert, X. and Courcelle, E. (2003) ESPript/ENDscript: extracting and rendering sequence and 3D information from atomic structures of proteins. Nucleic Acids Res. 31, 3320–3323.